Adsorption 9: 331–336, 2003

Sorption Behaviour of Molybdenum on Different Antimonates Ion Exchangers

I.M. EL-NAGGAR, E.A. MOWAFY, G.M. IBRAHIM AND H.F. ALY
Atomic Energy Authority, P.O. Code 13759, Cairo, Egypt

Received February 5, 2002; Revised May 19, 2003; Accepted June 3, 2003

Abstract. Various antimonate compounds are well known as important inorganic ion exchangers, since they resist radiation and chemical degradation and also exhibit selectivities towards different cations. Ceric, silicon, titanium and ferric antimonates were prepared as inorganic ion exchangers. Characterization of these materials has been described using different techniques, including thermal analysis, surface area measurements, X-ray diffraction and IR-spectroscopy. In batch distribution experiments the influence of HNO_3 molarity and Mo concentration for Mo sorption on different matrices is described in terms of their retention capacities and distribution coefficients.The selectivities of these exchangers towards molybdenum are in the order: CeSb > SiSb > FeSb > TiSb.

Keywords: antimonates, sorption, ion exchange, selectivity, molybdenum

Introduction

Radioisotopes play an important role in the peaceful uses of atomic energy. The radioisotope most widely used in medicine is technetium-99m, employed in more than half of all nuclear medicine procedures. It is an isotope of the artificially produced element technetium and it has almost ideal characteristics for a nuclear medicine scan. It has a half-life of six hours, which is long enough to examine metabolic processes yet short enough to minimize the radiation dose to the patient (Lederer et al., 1967). Technetium-99m decays by an isomeric process in which gamma rays and low energy electrons are emitted. Since there is no high-energy beta emission, the radiation dose to the patient is low. The low energy gamma rays it emits easily escape the human body and are accurately detected by a gamma camera. Once again the radiation dose to the patient is minimized (Boyd, 1982).

Since molybdenum-99m is the only source of short lived daughter, Tc-99m (Nair et al., 1992), the goal of this study was to develop a highly specific molybdenum separation method that would be used to get ^{99}Mo from a fission product mixture with exponentially high purity. This process will mainly depend on the properties of the separating materials used. Many investigators continue to look for new inorganic ion exchange materials whose special properties such as resistance to high temperature and radiation fields can be employed to advantage.

The synthesis of inorganic ion exchangers has been studied by various workers (Clearfield, 1982). In a previous work, a number of new inorganic ion exchangers which have useful properties were prepared. These prepared compounds have been found to be very useful in various radioisotopes separation (El-Naggar et al., 1994, 2002a, 2002b). Antimonate exchangers have been studied first by Abe and Ito (1967); cation exchange materials which contain antimony have very high hydrolytic stability in nitric acid (Pospelov et al., 1975) and show selective radionuclide uptake (Ibrahim, 2001) as well as actinides (El-Naggar et al., 1997) from nitric acid solutions. In this contribution, four different antimonates ion exchangers (ceric, silicon, titanium and ferric antimonates) were prepared and characterized. The sorption behavior of molybdenum on these prepared antimonates ion exchangers were investigated. In this work we will describe the influence

of nitric acid molarity and molybdenum concentration for Mo sorption on different prepared ion exchangers in terms of their retention capacities and distribution coefficients.

Experimental

All chemicals used were of analytical reagent purity grade and used without further purification.

Preparation of Antimonates Ion Exchangers

The four ion exchangers, titanium, ceric, silicon and ferric antimonates used in our investigation were prepared and purified in our laboratories as the following: 0.6 M solution of antimony metal was and mixed dissolved in aqua regia with equimolar solutions of titanium(IV) chloride, sodium metasilicate, ferric nitrate or ammonium ceric nitrate. The mixtures were aged overnight in the mother liquor to get complete digestion of the components followed by precipitation with either bidistilled water or liquid ammonia solution. The precipitates were washed using 1 M HNO_3 to remove Cl^- ions then rewashed by bidistilled water to remove NO_3^-. The products were centrifuged, air dried at 50°C, ground and sieved to the required mesh sizes and finally air dried at room temperature (Aly et al., 1998; El-Naggar and Aly, 1994, 1995; Aly and El-Naggar, 1998; El-Naggar et al., 2000).

The skeletal structures of the product exchangers were tested by infrared spectrometry. IR spectra were recorded with a Bomem FTIR spectrometer using KBr disk technique in the range 400–4000 cm^{-1}. The specific surface area and porosity measurements were achieved using BET-technique as an adsorption phenomenon of nitrogen gas on the powder surface at 77 K by means of NOVA A 3200, Quantachrome Corp., USA. Simultaneous differential thermal analysis and thermogravimetric analysis was used to follow up both phase changes and weight loss in the prepared exchangers at different temperatures. These analyses were carried out using a Shimadzu DTG-40 thermal analyzer obtained from Shimadzu Kyoto, Japan. The samples measured from ambient temperature up to 650°C with a heating rate of 10 deg/min. The apparent capacity of the prepared exchangers for molybdenum was determined by repeated bath equilibration of the exchanger with molybdenum solutions at different concentrations and pH values. Also, the capacity of the above mentioned exchangers was determined at different drying temperatures (50, 200 and 400°C). The capacity in mmole/g was calculated from the following formula;

$$\text{Capacity (meq./g)} = \frac{\%\ \text{uptake}}{100} \times C_o \times \frac{v}{m}$$

where, C_o: the initial concentration of solution (M), v: the solution volume (ml), and m: the weight of the exchanger (g).

The building temperatures of the new-formed phases were successfully detected by X-ray diffraction (XRD) techinque using a Shimdzu X-ray diffractometer, model XD 610, with a nickel filter and Cu-K_α radiation. The ion exchange behavior of the prepared exchangers towards Mo(VI) was detected by application of the thiocyanate method under different conditions (Basset et al., 1985), using single beam spectrophotometer at 465 nm.

Results and Discussion

The chemical stability of the prepared materials was previously studied (El-Naggar et al., 2000). The chemical stability of the studied matrices in H_2O, HNO_3 and HCl follows the order;

$$\text{FeSb} > \text{SiSb} > \text{CeSb} > \text{TiSb}.$$

Characterization of the Prepared Exchangers

The prepared antimonate exchangers were characterized using different analytical techniques such as XRD, FTIR and DTA-TG analyses as reported earlier (El-Naggar et al., 2000). The Figures are not given here for sake of brevity.

The skeletal structures of different antimonates were defined using infrared spectrometry, by means of FTIR . The metal-oxygen characteristic band in the wave number range between 700–900 cm^{-1} is independent of the drying temperature. On the other hand, the two bands nearly at 1615–1634 and 3400–3600 cm^{-1}, characteristic for interstitial water with strong H-bonding are highly affected by heat treatment of the prepared exchangers. As the drying temperature increases from 50°C to 850°C, passing through 200, 400 and 650°C, the intensities of these peaks gradually decrease and completely diminish at 850°C. These data reflect the complete loss of water at 850°C.

Simultaneous differential thermal analysis and thermogravimetry were used to study phase

Table 1. Weight loss % of the different prepared ion exchangers as a function of temperatures.

	Exchanger			
	Weight loss %			
Temp. (°C)	CeSb	FeSb	SiSb	TiSb
200	5.87	2.03	5.06	10.44
400	11.04	8.25	9.99	29.96
650	14.26	11.98	15.71	31.75
850	15.23	13.22	18.82	32.53

transformations and weight loss during heat treatment. The measurements were carried out at a heating rate of 10 K/min. to attain equilibrium temperatures. The curves showed that the endothermic peaks between 50–70°C were judged to be due to the loss of free water, while those appearing between 260–300°C were due to the loss of chemically bonded water. The exothermic peaks starting at 400°C may be attributed to metal oxide formation. In the case of silicon antimonate exchanger, a semicrystalline structure was obtained by drying at 50°C only.

The weight losses for the different exchangers at different drying temperatures are shown in Table 1. These weight losses correspond to the water content reduction of the exchangers at these temperatures.

The powder XRD patterns for the synthesized exchangers at different drying temperatures indicated that all materials prepared at 50°C are amorphous except for silicon antimonate, which shows some crystallinity at 50°C. By increasing the heating temperatures, the crystallinity begins to improve until it becomes more distinct at 850°C for all samples. The increase in crystallinity probably is a result of both dehydration and formation of hydrous metal oxides as indicated from DTA and TG curves. The change in crystallinity after thermal treatment is reported (Shuddhodan and Srinivasu, 1993).

The total surface area of the prepared exchangers was measured using the standard volumetric method by nitrogen gas adsorption at 77 K and application of the BET-equation. The equilibrium conditions of the adsorption process could be attained fairly rapidly and successive measurements were carried out at intervals of 30 min. to establish good reproducibility of the results. The values of the specific surface area in m^2/g and degree of porosity for the different exchangers were measured at 50, 200 and 400°C and represented in Table 2.

In case of ceric antimonate and ferric antimonate exchangers, the specific surface area and porosity increase with increasing the drying temperature. This may be attributed to the loss of water molecules, which occupy most of the reactive pores present in the exchangers. However, the specific surface area and, in turn, the porosity of the semi-crystalline silicon antimonate, dried at 50°C were found to be less than both of the same exchanger dried at 200 and 400°C.

On the other hand, titanium antimonate, dried at 200°C has a specific surface area lower than that obtained at 50 and 400°C. This may be attributed to the formation of the new crystalline phases before 400°C as indicated by DTA-TG and XRD measurements. The porosity values of these series were close to each other.

Apparent Capacity Measurements

The equilibrium time for sorption of 10^{-3} M Mo concentration on different antimonates is shown in Fig. 1. The figure shows that overnight standing is sufficient to attain equilibrium for Mo sorption on these matrices.

A comparison of the retention behaviour of these four matrices seemed a practical way to find a suitable sorbent for the sorption of the various molybdenum ions in acidified solutions depending on pH value and

Table 2. Specific surface area and porosity of the different prepared ion exchangers at different drying temperatures.

	Exchanger							
	CeSb		FeSb		SiSb		TiSb	
Tem. (°C)	Surface area (m^2/g)	Porosity (%)	Surface area (m^2/g)	Porosity (%)	Surface area (m^2/g)	Porosity (%)	Surface area (m^2/g)	Porosity (%)
50	47.8	20.7	10.1	8.2	23.1	15.14	23.5	12.11
200	78.5	40.2	17.9	16.8	64.5	21.06	10.8	13.2
400	77.9	47.55	23.6	22.2	55.7	21.55	20.12	15.32

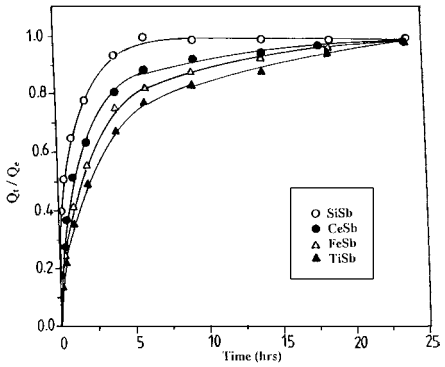

Figure 1. Effect of contact time for sorption of 10^{-3} M Mo on different antimonates at pH 3.07.

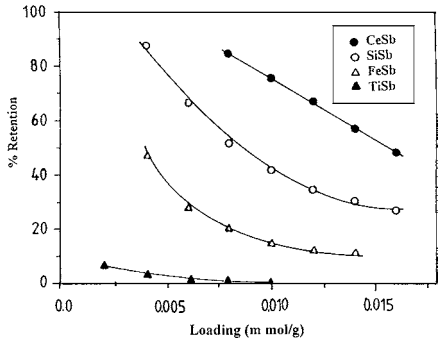

Figure 2. Relation of Mo retention against the loading on different antimonates at pH 2.5.

Mo concentrations (Shuddhodan and Srinivasu, 1993; Arino and Kramer, 1978):

$$MoO_4^{2-} \xrightarrow{pH=6} Mo_7O_{24}^{6-} \xrightarrow{pH=1.5} Mo_8O_{26}^{4-}$$

$$\xrightarrow{pH=0.9} MoO_3{\cdot}H_2O \xrightarrow{H^+} MoO_2^{2+}$$

Figure 2 shows the percent of Mo retention of these sorbents in pH 2.5 as a function of the loading, which is given by the ratio: amount of Mo to be adsorbed /weight of dry ion exchanger. Figure 2 shows that the order retention on these sorbents for Mo loading is; CeSb > SiSb > FeSb > TiSb, which may be due to the heighest porosity and surface area values for CeSb (Table 2) compared to the other sorbents.

Figure 3 clarifies the relation between capacities and Mo ion concentration, which shows that as the molybdenum concentration increases, the capacity increases for CeSb, FeSb and TiSb antimonates until 10^{-2} M molybdenum concentration, while it remains nearly constant above this value. In case of SiSb, there also an

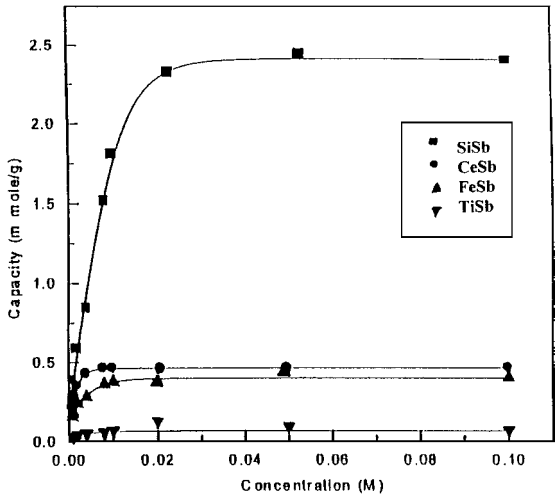

Figure 3. Effect of molybdenum concentration on the capacity of different antimonates, pH = 2.7.

increase in the capacity for molybdenum with the increase of molybdenum concentration, but the capacity remains constant after 3×10^{-2} M molybdenum concentration. Also, Fig. 3 shows that silicon antimonate has the highest capacity values for the molybdenum among the other exchangers and this is obvious result since silicon antimonate has a crystal structure which permits the selectivity of SiSb for molybdenum to be higher than that of the other exchangers. The selectivity order for Mo towards the studied matrices is SiSb > CeSb > FeSb > TiSb. The increase in the capacity as a result of increasing Mo concentration is expected since the increase in concentration may be due to the increase in the number of exchangeable sites.

The variation in the capacity of the exchangers to molybdenum with the equilibrium pH is presented in Fig. 4, which shows that for CeSb, FeSb and SiSb as the equilibrium pH increases, the capacity increases until a definite value of pH, after which the capacity decreases with increase in equilibrium pH. At low pH values, Mo (VI) is present in an equilibrium mixture of different polymeric forms; the predominance of any one of these forms is a function of the molybdenum and acid concentration (Burck et al., 1988). However, the adsorption of molybdenum on the different exchangers can be attributed to the attraction of the negatively charged molybdate ions in the solution to the positively charged sites of the exchangers, which depend to a great extent on H^+. Polymeric molybdate forms which have high negative charges will compete with those of lower

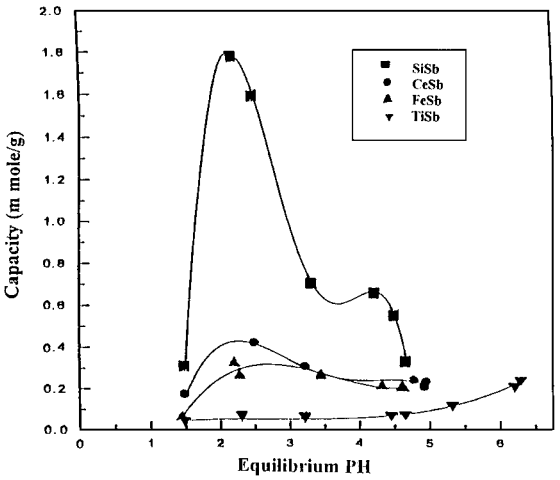

Figure 4. Effect of equilibrium pH on the capacity of different antimonates, [Mo] = 10^{-2} M.

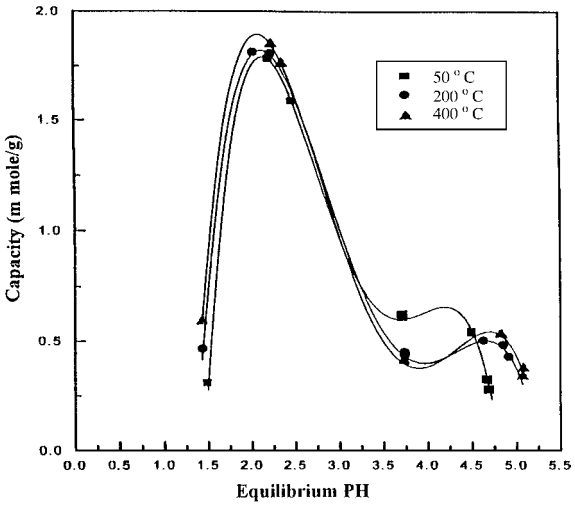

Figure 5. Effect of equilibrium pH on the capacity of SiSb dried at different temperatures, [Mo] = 10^{-2} M.

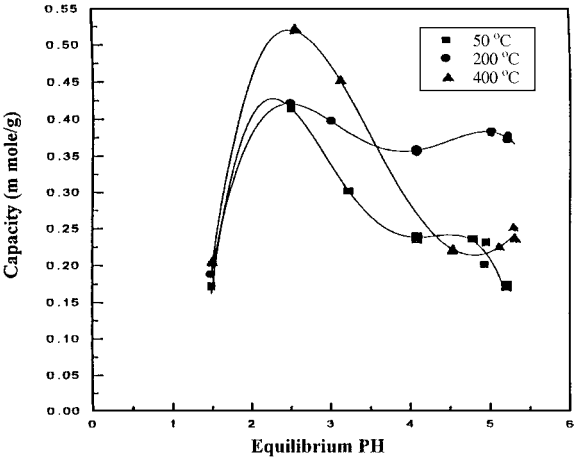

Figure 6. Effect of equilibrium pH on the capacity of CeSb dried at different temperatures, [Mo] = 10^{-2} M.

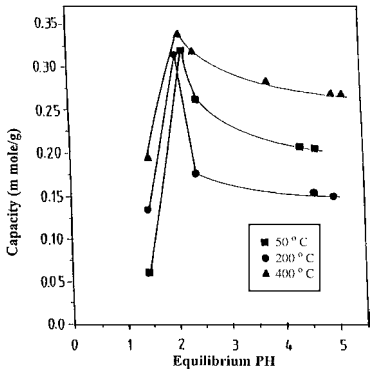

Figure 7. Effect of equilibrium pH on the capacity of FeSb dried at different temperatures, [Mo] = 10^{-2} M.

negative charge species. So, at lower pH values the capacities of the above exchangers for molybdenum are of small values since the predominant species of molybdenum has a small negative charge value. As the pH increases above 1.5, the capacities begin to increase due to the formation of the highly charged species, $[Mo_7O_{24}]^{6-}$. With further pH increase, the concentration of H^+ ions decreases leading to a decrease in the positively charged sites of the exchangers and so to a weak interaction between the molybdenum and the exchangers surface, leading to a decrease in the capacity values. In case of TiSb, the behavior is somewhat different since TiSb exhibits amphoteric behavior (Ibrahim, 2001). Therefore, as the pH increases the concentration of OH^- will increase and so the anionic species of molybdenum will exchange with the OH^- ions. So, as the pH increases the capacity will increase.

With respect to the effect of drying temperatures on the capacities, it appears from Figs. 5–8 that, the trend is different from one exchanger to another. In the case of CeSb and SiSb the capacity increases on drying at 200 and 400°C compared with that at 50°C and the values of capacity for the samples that were dried at 200 and 400°C are so close to each other, as shown in Figs. 5 and 6. These results depend to great extent on the values of porosity that are summerized in Table 2 since the values of porosity increased on drying from 50 to 200 and 400°C, while the values of porosity are so close at 200 and 400°C. For TiSb as shown in Fig. 7, the drying temperatures have a small effect on the values of the capacity as these values are nearly equal to each other. This behaviour also agrees with the values of

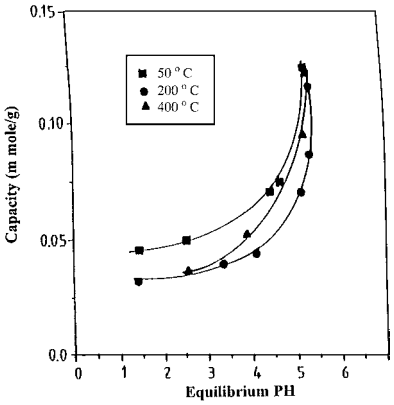

Figure 8. Effect of equilibrium pH on the capacity of TiSb dried at different temperatures, [Mo] = 10^{-2} M.

porosity which are not affected with drying temperature from 50 to 400°C. In case of FeSb, the behaviour is somewhat different since the capacity for the samples dried at 200°C is lower than that dried at 50 and 400°C, as shown in Fig. 8. The decrease in capacity at 200°C is attributed to the loss of water molecules, which may act as exchangeable active sites in the exchanger, while the increase in capacity again at 400°C is attributed to shrinkage in the crystal lattice permitting the formation of new active sites.

References

Abe, M. and T. Ito, *Kogyo Kagaku Zasshi*, **70**, 440 (1967).

Aly, H.F. and I.M. El-Naggar, *J. Radioanal. Nucl. Chem.*, **228**, 151 (1998).

Aly, H.F., E.S. Zakaria, and I.M. El-Naggar, *Colloids and Surfaces*, **131**, 33 (1998).

Arino, H. and H.H. Kramer, *J. Applied Radiation and Isotopes*, **29**, 97–102 (1978).

Basset, J., R.C. Denney, G.H. Jeffery, and J. Mendham, "Vogels Text Book of Quantitative Inorganic Analysis," 4th ed., 1985.

Boyd, R.E., *Radiochim. Acta*, **30**, 123 (1982).

Burck, J., S.A. Ali, and H. Achc, *J. Solv. Extr. and Ion Exch.*, **6**, 167 (1988).

Clearfield, A., *Inorganic Ion Exchange Materials*, CRC Press, Inc., Boc Raton, FI, 1982.

El-Naggar, I.M., M.M. Abdel-Hamid, and H.F. Aly, *Solv. Extr. Ion Exch.*, **12**(3), 651 (1994).

El-Naggar, I.M. and H.F. Aly, Progress Report Submitted to IAEA, Research Contract No. 7213, RB (1994–1995).

El-Naggar, I.M., E.S. Zakaria, G.M. Ibrahim, and H.F. Aly, *Egyptian J. Analytical Chem.*, **6**, 153 (1997).

El-Naggar, I.M., E.A. Mowafy, and G.M. Ibrahim, *7th Conf. Nucl. Sci. & Appl.*, **1**(1), 75 (2000).

El-Naggar, I.M., M.M. Abdel-Hamid, E.A. Mowafy, S.A. Shady, and N. Belacy, *Arab J. Nucl. Sci. & Appl.*, **35**(3), 65 (2002a).

El-Naggar, I.M., E.A. Mowafy, I.M. Ali, and H.F. Aly, *J. Adsorption*, **8**(3), 565 (2002b).

Ibrahim, G.M., "Separation of Mo-99 from Fission Product by Exchange Technique in Aqueous and Organic Media," Ph.D. Thesis, Chemistry Dept., Faculty of Science, Cairo University, Egypt, 2001.

Lederer, C.M., J.M. Hollander, and I. Perlmarn, *Tables of Isotopes*, 6th ed., New York, 1967.

Nair, A.G.C., S.K. Das, S.M. Deshmukh, and Satya Prakash, "Carrier Free Separation of ^{99}Mo from ^{233}U Fission Products," *Radiochimica Acta* **57**, 29 (1992).

Pospelov, A.A., V.N. Krylov, G.N. Maslova, et al., Ecological Technology, "Ecological Technology in Non Ferrous Metallurgy," Inter Collegiate Collection (in Russian), Izd.UPI im, S.M. Kirova, Sverdlovsk, 63–68 (1975).

Shuddhodan, P. and N. Srinivasu, *Radiochemica. Acta*, **44**, 52 (1993).